Available online at www.sciencedirect.com

ScienceDirect

Procedia CIRP 45 (2016) 83 – 86

www.elsevier.com/locate/procedia

3rd CIRP Conference on Surface Integrity (CIRP CSI)

Increase of the coefficient of static friction using turn-milling with an inclined milling spindle

R. Funke*, A. Schubert

Professorship Micromanufacturing Technology, Technische Universität Chemnitz, 09107 Chemnitz, Germany

* Corresponding author. Tel.: +049 371 531 36969; fax: +049 371 531 836969. *E-mail address:* roman.funke@mb.tu-chemnitz.de

Abstract

There is a strong need for surfaces with a high coefficient of static friction to meet the demands for increasing performance and lightweight construction strategies, especially regarding friction-locked connections. An auspicious turn-milling process used to generate protruding surface structures which lead to a high coefficient of static friction is investigated. The influence of the corner geometry on the surface structure is examined by machining end faces of specimens of the steel 42CrMo4+QT (1.7225). Experimental tests for the identification of the coefficient of static friction show a significant increase up to 275 % ($\mu_{0.1°} = 0.55$) for turn-milled surfaces in comparison to unstructured specimens ($\mu_{0.1°} \approx 0.2$).

Peer-review under responsibility of the scientific committee of the 3rd CIRP Conference on Surface Integrity (CIRP CSI)

Keywords: Cutting; Static friction; Surface integrity; Tribology; Turn-milling

1. Introduction

The development of technical systems is characterised by increasing power densities as well as lightweight construction strategies. This also concerns machine elements for the transmission of forces and torques like friction-locked connections, e. g. flange joints, bolt connections and shaft to collar connections. A high coefficient of static friction is desired in such applications to permit lower tightening torques or a reduced number of bolts.

There are several approaches to increase the static friction of surfaces. In mechanical engineering, electroless nickel dispersion coatings are used. By embedding hard particles of SiC, tungsten carbide or diamond in the coating, values up to $\mu_0 = 0.6$ are attainable. The particles protrude out of the coating and generate a strong ploughing in the counter surface. Either the coating is applied directly on the workpiece or so called friction shims are assembled in the contact zone. The fields of application encompass the automotive industry and wind energy systems. Hammerström and Jacobson generated pyramidal surface structures and examined their influence on the frictional behaviour [1]. The surfaces were manufactured using micromechanical techniques based on photolithography, etching of silicon and subsequent deposition of CVD diamond. The sharp-edged structures also induce a strong ploughing component and values up to $\mu_0 = 1.2$ were achieved. Another approach is the surface texturing by laser ablation [2, 3]. Such surfaces are characterised by protruding structures caused by melting and ablation processes contributing to high friction. It could also be observed that laser machining leads to an increase of the surface hardness which seems to be beneficial for high coefficients of static friction.

The mentioned strategies represent additional processes that come along with higher costs and requirements for the quality management. This paper shows an approach to increase the coefficient of static friction by surface structuring during the cutting process without any subsequent processes. Turn-milling with an inclined milling spindle is used to create protruding sharp-edged surface structures leading to a clamping with the counter surface.

Peer-review under responsibility of the scientific committee of the 3rd CIRP Conference on Surface Integrity (CIRP CSI)
doi:10.1016/j.procir.2016.02.120

Nomenclature

a_p	Depth of cut
d_t	Tool diameter
d_w	Workpiece diameter
D_A	Outer diameter of the friction surface
D_I	Inner diameter of the friction surface
D_R	Friction diameter
f_{rad}	Radial feed per workpiece revolution
f_{ztan}	Feed per tooth in the tangential direction
F_N	Normal force
M_t	Friction torque
n_t	Rotational speed of the tool
n_w	Rotational speed of the workpiece
r_{eff}	Effective working radius
r_ε	Corner radius
Rt_{tan}	Kinematic roughness in the tangential direction
Sa	Arithmetic mean height
Sku	Kurtosis
Sp	Maximum peak height
Sq	Root mean square height
Ssk	Skewness
Sv	Maximum valley depth
Sz	Maximum height of the surface
v_c	Cutting speed
v_{frad}	Feed rate in the radial direction
v_{ftan}	Feed rate in the tangential direction
z_c	Number of teeth
β	Tool inclination angle
$\mu_{0.1°}$	Coefficient of static friction for $\varphi = 0.1°$
φ	Angle of twist

2. Experimental

2.1. Surface structuring by turn-milling

For the experiments, turn-milling of specimens of the heat treatable steel 42CrMo4+QT (1.7225) was carried out in order to determine the influence of the process parameters on the surface structure and the coefficient of static friction. The kinematics used is shown in Fig. 1. As a combination of turning and milling the engagement parameters cannot be assigned to one process clearly and had to be defined. The tool is inclined by an angle β relative to the face side. Similar to facing the feed motion runs towards the workpiece axis with the radial feed f_{rad} per workpiece revolution. However, due to the tool rotation there is an interrupted cut leading to deterministic structures (facets) at intervals of the feed per tooth f_{ztan} in the tangential direction corresponding to the circumferential direction. To keep the feed per tooth f_{ztan} and therewith the facet size constant, the rotational speed of the workpiece has to be adapted similar to face turning according to the effective working radius r_{eff}:

$$f_{ztan} = \frac{2 \cdot \pi \cdot r_{eff} \cdot n_w}{n_t \cdot z_c} = \frac{v_{ftan}}{n_t \cdot z_c}. \quad (1)$$

Obviously, it is not possible to machine the entire face side in that manner because of the restricted revolution speed of the workpiece. Thus, this process is predominantly suited for the machining of annular surfaces. In contrast to face-turning the peripheral speed of the workpiece at the point of the cutting edge engagement does not equate to the cutting speed but to the feed rate in the tangential direction v_{ftan} (Eq. 1). The cutting speed v_c is determined by the rotational speed n_t and diameter d_t of the tool. Concerning the cutting speed, the workpiece rotation can be neglected. Double-edged, TiAlN coated cemented carbide end milling cutters with four different corner geometries were used for the experiments: point (a), chamfer 0.2 mm x 45° (b), radius 0.2 mm (c) and point with a tool cutting edge angle of the minor cutting edge of 15° (d), Fig. 1. The latter is a special tool geometry which is not available by default. The objective was to create a steep flank angle of 90° (at $\beta = 15°$) within the surface profile to achieve a high ploughing in the counter body and a high resistance against a relative movement, Fig. 2 (d). The corner geometry determines the surface profile and the kinematic roughness in the tangential direction Rt_{tan}, Fig. 2. For all experiments minimum quantity lubrication with polyol ester with a flow rate of 25 ml per hour was used. The process parameters applied are presented in Table 1.

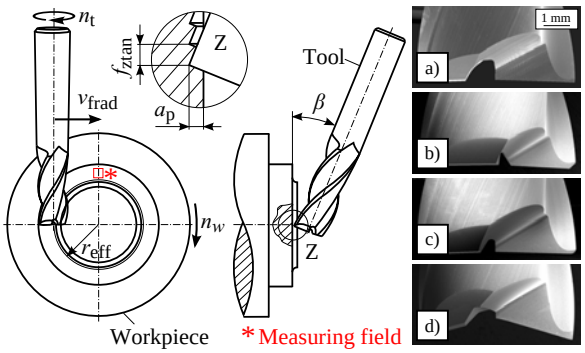

Fig. 1. Process kinematics and examined corner geometries: Point (a), Chamfer (b), Radius (c), Point 15° (d)

Table 1. Experimental settings

Parameter	Value	Unit
Feed per tooth f_{ztan}	0.2	mm
Radial feed f_{rad}	0.3	mm
Cutting speed v_c	150	$m \cdot min^{-1}$
Depth of cut a_p	0.2	mm
Tool inclination angle β	15	1°
Tool diameter d_t	6	mm

2.2. Measurement of surfaces

A tactile roughness measurement of the machined structures is not possible because the flanks of the profile are too steep. Furthermore, the anisotropy of the facets does not allow the measurement of a line roughness. Therefore an optical 3D laser scanning microscope Keyence VK-9700 was used for measuring details with a size of (2 x 2) mm^2, Fig. 1. The analysis of the measuring data was conducted with the software MountainsMap® 6.2. The obtained surface data was corrected

due to inclination and a median filter was used for noise reduction.

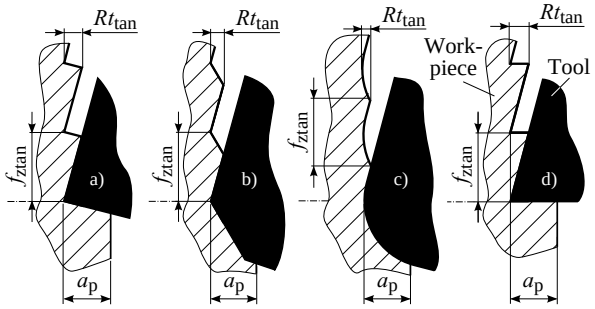

Fig. 2. Resulting surface profile and kinematic roughness Rt_{tan} in the tangential feed direction for different corner geometries (β = 15°): Point (a), Chamfer (b), Radius (c), Point 15° (d)

2.3. Tribological evaluation

For the determination of the coefficient of static friction a special test rig of the Institute of Design Engineering and Drive Technology at Technische Universität Chemnitz was used. In the test rig two specimens are arranged coaxially and contacted by their annular face sides with an inner diameter of D_I = 15 mm and an outer diameter of D_A = 30 mm, Fig. 3. A normal force F_N is applied in the axial direction and the specimens are twisted against each other at 0.5° per second. The angle of twist φ and the friction torque M_t are recorded at once. For all experiments a normal force of F_N = 53 kN (nominal pressure 100 MPa) was applied. The coefficient of static friction is calculated using the friction diameter D_R:

$$\mu_{0.1°} = \frac{2 \cdot M_t(\varphi = 0.1°)}{F_N \cdot D_R}, \quad (2) \qquad D_R = \frac{2}{3} \cdot \frac{D_A^3 - D_I^3}{D_A^2 - D_I^2}. \quad (3)$$

For all tests the coefficient of static friction $\mu_{0.1°}$ for a permissible torsion angle of 0.1° was determined, Fig. 3. A detailed description of the test procedure can be found in [4]. For the counter bodies, specimens of the steel C45 (1.0503) were face-turned with a C-formed indexable insert with r_ε = 0.4 mm and f = 0.15 mm.

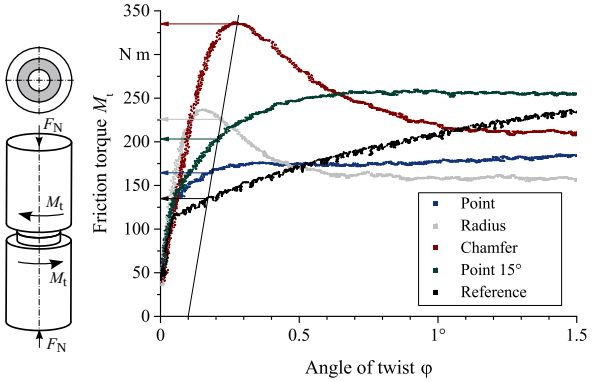

Fig. 3. Arrangement of specimens during friction test (left) and torque curves as a function of the corner geometry

Each parameter combination was tested five times. A pair of two unstructured specimens (C45 vs. 42CrMo4+QT) served as reference test. These specimens were face-turned with the same cutting parameters as described for the counter bodies. A mean value of $\mu_{0.1°}$ = 0.21 was determined for the reference test.

3. Results

3.1. Process simulation

In order to investigate the influence of the process parameters d_t, f_{ztan}, f_{rad}, β and the corner geometry on the resulting surface structure, a simulation model based on a dexel model was developed in Matlab®. During the programme run the tool is moved "through" an (m x n)-matrix of nodes of a defined length which represent the workpiece surface. The movement of the tool is divided into discrete steps dependent on the feed parameters f_{ztan} and f_{rad}. At every single step the penetration of the tool and the nodes is checked and the altitude of the nodes is reduced respectively. In the present case the tool is modelled as a rotationally symmetrical body whose contour equates to the circular movement of the cutting edges in a standard CAD software. The CAD model has to be converted into a 3D-point cloud and then can be imported into the Matlab® programme. The resulting surface can be exported as a point cloud and evaluated in MountainsMap®. A comparison of simulation and experiment is illustrated in Fig. 4. There is a good agreement concerning the qualitative surface structure as well as quantitative surface parameters.

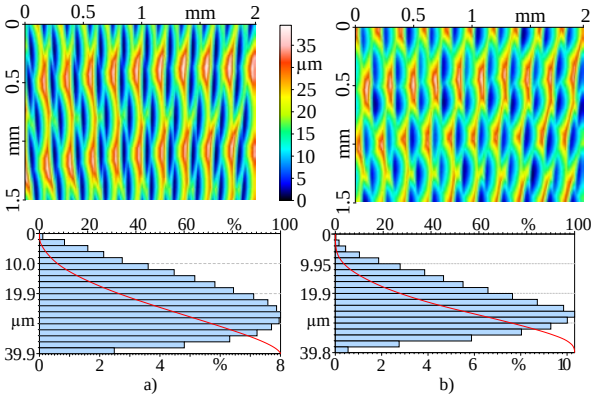

Fig. 4. Comparison of simulated (a) and machined (b) surface (chamfered corner)

3.2. Experimental results

The influence of the corner geometry on the coefficient of static friction is shown in Fig. 5. The bars represent the mean values of five rig tests at identical parameters. The error bars describe the minimum and the maximum values. All values for $\mu_{0.1°}$ are above the reference test using unstructured specimens. The highest values up to 0.55 were achieved with the chamfered corner. The appendant friction torque curves are illustrated in Fig. 3. There is a distinct peak in the curves generated with the rounded and the chamfered corner.

Table 2 presents the correlation coefficients between some selected measured surface parameters and the coefficient of static friction. As expected a clear correlation cannot be verified. It can be stated, that there is a slight tendency that lower values of *Sz* and *Sp* lead to a higher values of $\mu_{0.1°}$.

Table 2. Correlation of areal parameters and $\mu_{0.1°}$

	Sq	*Sa*	*Sp*	*Sv*	*Sz*	*Ssk*	*Sku*
Correlation coefficient	-0.54	-0.54	-0.66	-0.51	-0.63	-0.14	-0.16

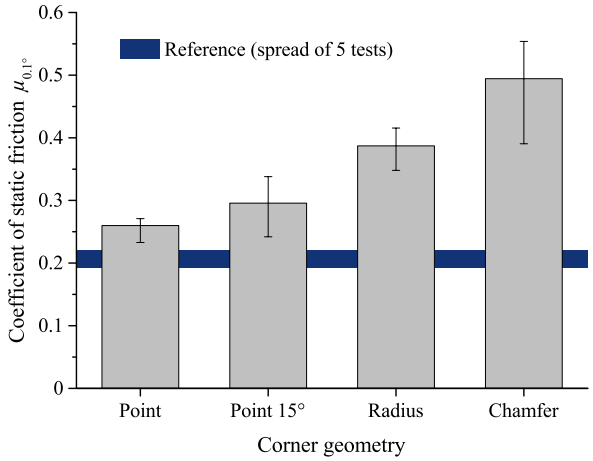

Fig. 5. Influence of the corner geometry on the coefficient of static friction

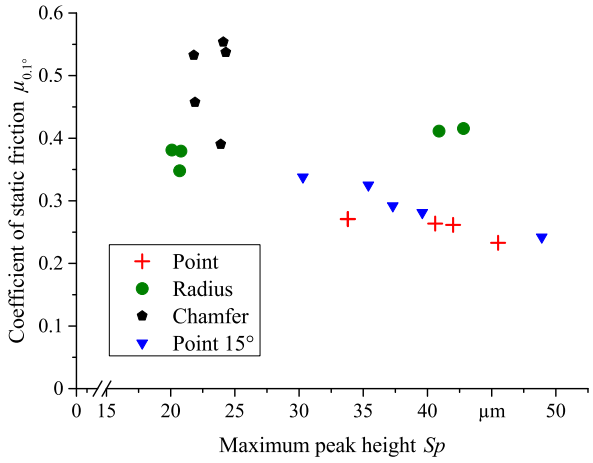

Fig. 6. Correlation between maximum peak height *Sp* and the coefficient of static friction $\mu_{0.1°}$

The values for the measured maximum peak height *Sp* and the appropriate coefficient of static friction of all experiments are illustrated in Fig. 6. There are significant differences between the values within certain test series. The causes are not fully understood yet. First of all there is always a geometrical deviation between the cutting edges using multiple-edged tools. This results in higher roughness values for cutting tools in mint condition. During the cutting process the geometry of the cutting edges approximates due to the increasing tool wear. A radial runout and vibrations of the tool are further causes, superimposed to the priorly mentioned effects. Beyond that a chipping of the tool corner results in increased roughness values.

To understand the effective friction mechanisms in the contact zone it is necessary to examine the surfaces after the rig test. In Fig. 7 the structured surface which generated the highest coefficient of static friction and the appendant counter surface are presented. It can be seen that the structures had penetrated into the counter surface. During twisting the structures induce a strong ploughing until the peaks are being sheared-off. This is in good agreement with the friction torque curve in Fig. 3.

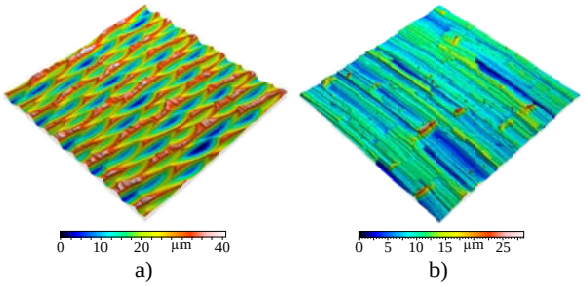

Fig. 7. Structured surface (corner geometry: chamfer) (a) and counter surface (b) after rig test

4. Summary and conclusions

A developed dexel-based Matlab® simulation model permits a qualitative and quantitative prediction of the surface geometry and the evaluation of specific areal surface parameters. The influence of the tool corner geometry on the surface structure and the coefficient of static friction was investigated. In all experiments an increase of the coefficient of static friction $\mu_{0.1°}$ could be achieved in comparison to unstructured surfaces. For $\mu_{0.1°}$ values up to 0.55 were achieved with a chamfered corner. Thus, the values are comparable to that achieved when using friction shims.

Further experiments will focus on the influence of the feed components on the surface structure and the coefficient of static friction. Furthermore, the influence of cutting speed and tool wear on the structure and the hardness of the external zone and its influence on the frictional behaviour have to be determined.

References

[1] Hammerström L, Jacobson S. Designed high-friction surfaces – Influence of roughness and deformation of the counter surface. Wear 2008; 264:807-814

[2] Dunn A, Carstensen J V, Wlodarczyk K L, Hansen E B, Gabzdyl J, Harrison P M, Shephard J D, Hand D P. Nanosecond laser texturing for high friction applications. J Optics and Lasers in Engineering 2014;62:9-16.

[3] Flores G, Wiens A. Mit dem Laserstrahl die Haftreibung erhöhen. wb Werkstatt und Betrieb 2013; 7-8:102-106

[4] Schuller S; Leidich E. Haftreibwerte. Ermittlung von Haftreibungszahlen und Reibungscharakteristiken sowie deren Einflussparametern auf Basis eines neuen Standardprüfverfahrens. Abschlussbericht FVV 2010, 906